

Coalescence Dynamics of Two Liquid Droplets

R. Li[†], N. Ashgriz^{*} and S. Chandra

Department of Mechanical and Industrial Engineering
University of Toronto
Ontario, M5S 3G8, Canada

Abstract

We present an experimental study on the coalescence of a falling droplet with a stationary sessile droplet on a solid surface under isothermal condition. High speed video images are presented to show coalescence dynamics, shape evolution and contact line movement. The contact line movement is found related to the change of local dynamic contact angle and evolution of free surface. The motion of contact line also affects the evolution of spread length, which is the length along the centers of the two droplets. Experimental observations show that the spread length could be larger or smaller than ideal spread length, which is the spread diameter of individual droplet plus the center-to-center spacing of the two droplets. Three coalescence mechanisms are observed and identified comparing maximum and minimum spread lengths to the ideal spread length during coalescence.

Introduction

Controlled deposition of droplets on solid surfaces is used in a number of industrial applications such as solid-inkjet printing [1], micro-fabrication [2], rapid prototyping [3] and electronic packaging [4,5]. These applications require accurate placement of molten wax, polymer or metal droplets on substrates to build images, three-dimensional parts or electrically conductive lines. Neighboring droplets need to overlap and coalesce during impact process. Fluid interactions between droplets may displace droplets, and unpredictable movements of droplets may make lines break or vary in thickness [6-8]. There is lack of basic understanding about the coalescence of droplets during deposition. In most of early studies on droplets coalescence [9-14], the initial kinetic energy of droplets was very low, and the velocity of approach between droplets was usually taken to be zero. Additionally, emphasis was put on the early-time behavior of the interface between droplets, which is dominated by surface tension and viscosity.

We studied the coalescence of a falling droplet with a stationary sessile droplet on a solid surface under isothermal condition, as shown in Fig. 1. Two droplets with the same initial diameter D_0 and impact velocity U are deposited sequentially with center-to-center spacing L . The first droplet is static when the second droplet impacts (Fig. 1a). If the second droplet touches the first during impact, the two droplets coalesce (Fig. 1b). In our experiments we observed the motion of the liquid-solid contact line and developed correlations to predict the final spread length, D_y , of the coalesced droplets, which is the length of liquid along the axis joining the centers of the two drops (Fig. 1b).

Experimental Method

Droplet coalescence dynamics were recorded using a high speed video camera (FASTCAM-ultima 1024, Photron Ltd.). Two liquids were used, distilled water ($\rho=998\text{ kg/m}^3$, $\mu=1\text{ cP}$, $\sigma=73\text{ dyne/cm}$) and ethylene glycol ($\rho=1113\text{ kg/m}^3$, $\mu=16\text{ cP}$, $\sigma=47\text{ dyne/cm}$). Properties of the two liquids are given in Table-1. In our tests, the sizes of water and ethylene glycol droplets D_0 were 1 - 2 mm in diameter. Velocity U was varied from 0.3 to 1 m/s. The coalescence of two liquid droplets occurs in two stages: the first phase is inertia driven, while the second is a spontaneous relaxation toward equilibrium. In the present work, we focus on the inertia driven phase.

The variation in spread length D_y is measured for 25 ms after the impact of the second droplet. From measurement of D_y , maximum and minimum spread lengths, $D_{y,\max}$ and $D_{y,\min}$, can be determined (see Fig. 1c and 1d). Attention is also paid to the spreading and retraction of the far edges of coalescing droplets. From the high speed video images, the maximum spread point for each edge can be found, which is the farthest point the edge can reach during deposition. Then the displacements of the two edges relative to their maximum spread points are measured, d_L for left edge and d_R for right edge (see Fig. 1b and 1c).

[†] Current address: Thermal System Lab, GE Global Research, One Research Circle, Niskayuna, NY 12309, USA

^{*}Corresponding author

To quantify the overlap between droplets, the overlap ratio is defined as

$$\lambda = 1 - L/D_s \quad (1)$$

If $L=0$, $\lambda=1$, indicating that the second droplet is deposited directly over the first, while the droplets are just touching if $L=D_s$ so that $\lambda=0$. If we assume that the first droplet has no influence on the spread of the first, and there is no interaction between them, the ideal spread length is

$$D_{y,I} = D_s + L \quad (2)$$

This length is ideal because it could provide a consistent overlap condition (constant value of λ) between neighbor droplets when a number of droplets are deposited sequentially with equal spacing on a solid surface.

The deviation of actual spread length D_y from the ideal spread length $D_{y,I}$ will affect the relative location and coalescence of subsequent droplets with the first two droplets, and therefore is of importance to engineering applications based on multiple droplets deposition. In view of this, a non-dimensional spread length is defined as

$$\psi = D_y / (D_s + L) \quad (3)$$

Following this normalization scheme, the dimensionless, ideal spread length is

$$\psi_I = 1 \quad (4)$$

Following the normalization scheme defined above, the non-dimensional maximum spread length (ψ_{\max}) and minimum spread length (ψ_{\min}) are defined as

$$\psi_{\max} = D_{y,\max} / (D_s + L) \quad (5)$$

$$\psi_{\min} = D_{y,\min} / (D_s + L) \quad (6)$$

Similarly, the non-dimensional displacements of the left and right edges can be defined by

$$\chi_{L,R} = |d_{L,R}| / (D_s + L) \quad (7)$$

Results and Discussion

Experimental tests are conducted to observe the coalescence of two droplets on the stainless steel surface. Coalescence dynamics can be observed from time resolved images. Measuring the images provides the time evolutions of edge displacement and spread length. This section presents three types of coalescence dynamics showing different evolution mechanisms of spread length.

Case I: Figure 2a shows successive stages during the impact of two water droplets on a steel surface for a time period of 25 ms. The first droplet is at its equilibrium position when the second droplet impacts. For both droplets $We = \rho D_0 U^2 / \sigma = 8$, $Re = \rho D_0 U / \mu = 990$, and overlap ratio $\lambda = 0.39$. Figure 2b shows the displacements of the right and left edges relative to their maximum points. As the definition of $\chi_{L,R}$ (Eq. 7) suggests, a downward trend indicates spreading, while an upward trend indicates retraction. The left edge retracts earlier more than the right edge. Figure 2c shows the variation of spread length ψ with time. The spread length increases and exceeds the ideal spread length, reaching a maximum spread length $\psi_{\max} > 1$. The retraction of contact line causes the spread length to decrease, reaching a plateau value $\psi_{\min} < 1$.

To explain the dynamics of contact line, local dynamic contact angles at the two edges are measured and shown in Fig. 3a. Additionally, Figs. 3b displays enlarged pictures to show the curvature of free surfaces and contact angles at several instants. When approaching maximum spread, the free surface near the left edge has a small radius of curvature ($t \sim 2.5$ ms in Fig. 3b), creating high fluid pressure locally. The pressure creates internal flow away from the edge, decreasing the contact angle and making the contact line at the left edge retract. The left edge starts withdrawing at $t = 5.5$ ms (see Fig. 2b), and the contact angle reaches a minimum $\sim 20^\circ$ at $t = 7.5$ ms (see Figs. 3a and 3b). Afterwards, high pressure develops near the right edge due to the evolution of local free surface ($t \sim 8.5$ ms in Fig. 3b). As a result, the right edge starts retracting at $t \sim 9.5$ ms (see Fig. 2b), while the local contact angle decreases to $\sim 15^\circ$ at $t = 10.5$ ms (see Figs. 3a and 3b). The pressure change keeps alternating between the two edges, while the pressure difference decreases with increasing time due to viscous dissipation. This can be verified by the damping oscillations of the contact angles at the two edges as shown in Fig. 3a. For $t > 20$ ms, although the oscillation of drop shape is still visible (see Fig. 2a), the right and left edges are pinned (see Fig. 2b).

Case II: Figure 4 shows the coalescence of two water droplets with $We = 8$, $Re = 990$ and $\lambda = 0.86$. In Fig. 4a, the second droplet impacts and merges with the first droplet without touching the substrate surface. The inertia of the second droplet drives the merged drop to spread and oscillate on the surface. The displacements of the two edges are plotted in Fig. 4b, showing larger displacement for the left edge. Due to the large overlap ratio in this case $\lambda = 0.86$, there is

no significant time delay between the retractions of the two edges (compare Fig. 4b to Fig. 2b). Following the first retraction, the two edges repeat spreading and retraction with decreasing amplitudes. This causes ψ to oscillate with decreasing amplitude as shown in Fig. 4c. In this case, the maximum spread length is larger than the ideal length since $\psi_{\max} > 1$. The contact line retraction at the two edges causes significant decrease of spread length during the first oscillation. However, different from the previous case, the minimum spread length is still larger than the ideal length $\psi_{\min} > 1$.

Case III: In the previous two cases, the maximum spread length ψ_{\max} was measured to be larger than ψ_I . This is not always the case. Figure 5 shows the coalescence of two ethylene glycol droplets with $We=2.4$, $Re=30$ and $\lambda=0.31$. The second droplet impacts the steel surface and merges with the first droplet when spreading on the surface (Fig. 5a). The left edge retracts from the maximum spreading point with a small extent, while the right edge neither spreads nor retracts (Fig. 5b). Figure 5c shows that the spread length increases to a maximum and then slightly decreases to a plateau. In this case, the spread length remains smaller than the ideal length since $\psi_{\max} < 1$.

We have observed that during coalescence the spread length ψ may be larger or smaller than the ideal length ψ_I . Based on the relative magnitudes of ψ_{\max} and ψ_{\min} compared to ψ_I , three different types of coalescence of two droplets on a solid surface can be identified. The three mechanisms are schematically shown in Fig. 6 and correspond to the experimental cases reported in the previous section. In Fig. 6a, the two droplets spread beyond the ideal spread length at maximum spread extent ($\psi_{\max} > \psi_I$), after which surface tension forces pull the two edges back, making the minimum spread length less than the ideal spread length ($\psi_{\min} < \psi_I$). This coalescence mechanism is referred to as *drawback due to retraction*, which applies to Case I shown in Fig. 2. In Fig. 6b, the maximum spread length is larger than the ideal spread length, $\psi_{\max} > \psi_I$. If the surface tension forces are not strong enough to overcome viscous forces, the contact lines at the two edges may retract slightly or may not retract at all. Consequently, the minimal spread length is still larger than the ideal spread length, $\psi_{\min} > \psi_I$. This coalescence mechanism is referred to as *additional spread*, which applies to Case II shown in Fig. 4. Figure 6c shows another mechanism, in which the spread length never exceeds the ideal spread length. This mechanism is referred to as *drawback not due to retraction*, which applies to Case III shown in Fig. 5.

References

1. Snyder, T. and Korol, S., "Modeling the offset solid-ink printing process," *IS&T's Recent Progress in Ink Jet Technologies II*, 175-181 (1999).
2. Fang, M., Chandra, S. and Park, C.B., *Journal of Manufacturing Science and Engineering* 129:311-318 (2007).
3. Zhang, Y.-M., Chen, Y., Li, P. and Male, A.T., *Journal of Materials Processing Technology* 135:347-357 (2003).
4. Sirringhaus, H., Kawase, T., Friend, R.H., Shimoda, T., Inbasekaran, M., Wu, W. and Woo, E.P., *Science*, 290:2123-2126 (2000).
5. Liu, Q. and Orme, M., *Journal of Materials Processing Technology*, 115:271-283 (2001).
6. Gao, F. and Sonin, A.A., *Proceedings of the Royal Society of London, Series A* 44:533-554 (1994).
7. Duineveld, P.C., *Journal of Fluid Mechanics*, 477:175-200 (2003).
8. Li, R., Ashgriz, N., Chandra, S., Andrews, J.R., Williams, J., *Journal of Manufacturing Science and Engineering* 130:041011 (2008).
9. Ristenpart, W.D., McCalla, P.M., Roy, R.V. and Stone, H.A., *Physical Review Letters* 97:064501 (2006).
10. Menchaca-Rocha, A., Martinez-Davalos, A., and Nunez, R., *Physical Review E* 63:046309 (2001).
11. Thoroddsen, S.T., Takehara, K., and Etoh, T.G., *Journal of Fluid Mechanics* 527:85-114 (2005).
12. Andrieu, C., Beysens, D.A., Nikolayev, V.S., and Pomeau, Y., *Journal of Fluid Mechanics* 453:427-438 (2002).
13. Duchemin, L., Eggers, J. and Josserand, C., *Journal of Fluid Mechanics* 487:167-178 (2003).
14. Eggers, J., Lister, J. R., and Stone, H.A., *Journal of Fluid Mechanics* 401:293-310 (1999).

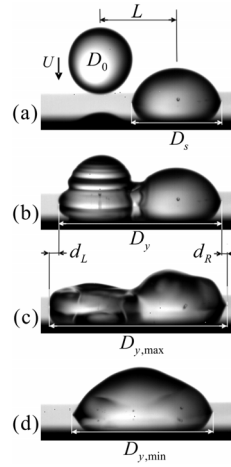


Figure 1: (a) Deposition of two droplets on a solid surface; (b) spread length D_y ; (c) maximum spread length $D_{y,max}$; (d) minimum spread length $D_{y,min}$.

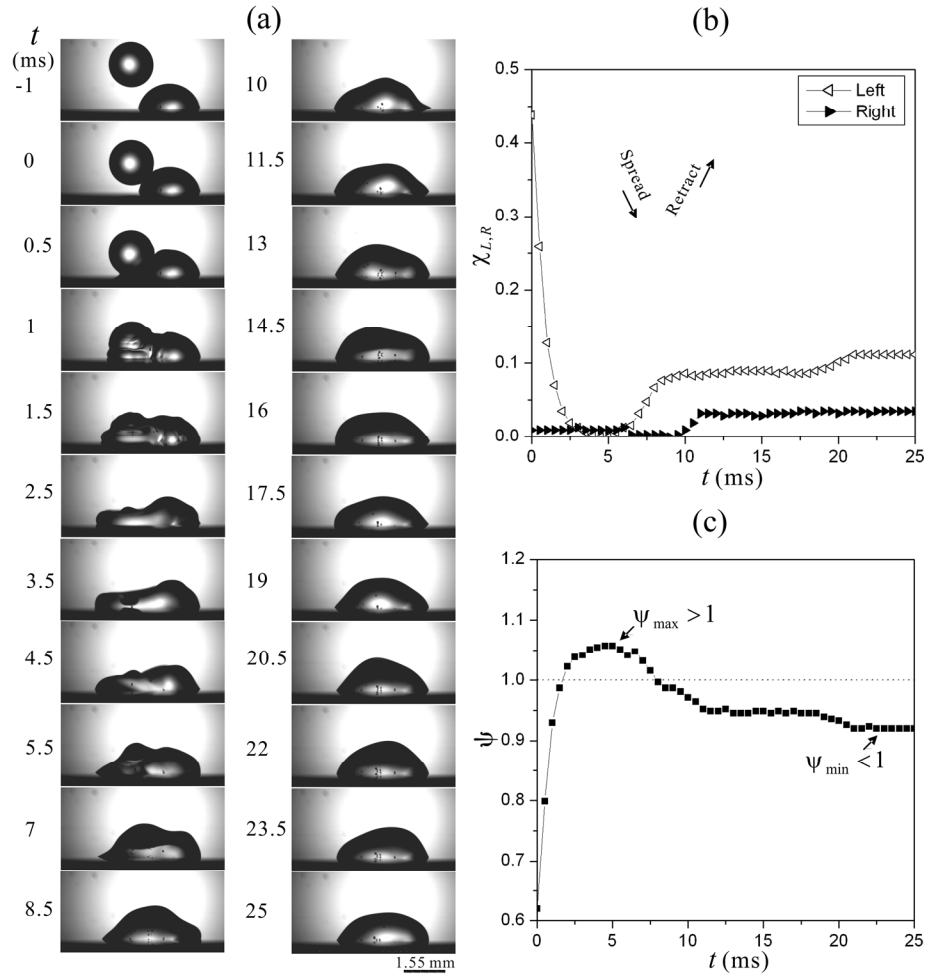


Figure 2: Coalescence of two water droplets on a stainless steel surface ($We=8$, $Re=990$, $\lambda=0.39$): (a) shape evolution; (b) edge displacements; (c) spread length evolution.

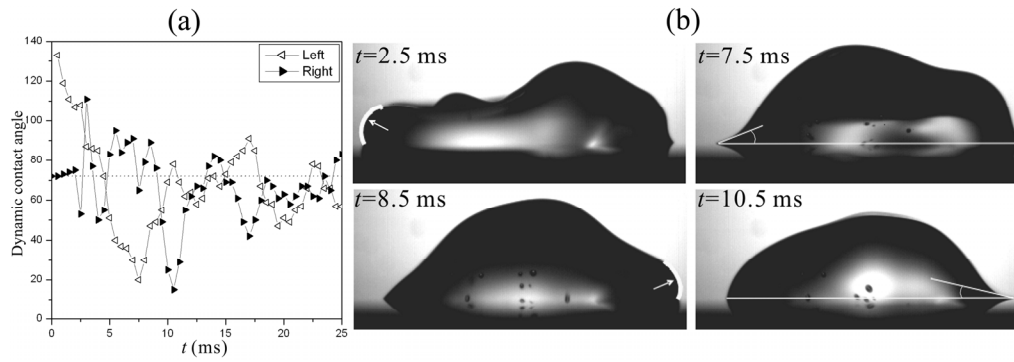


Figure 3: (a) Dynamic contact angle at left edge (2nd droplet) and right edge (1st droplet), corresponding to the test shown in Fig. 2. Dashed line: θ_s of 1st droplet prior to the impact of 2nd droplet. (b) Enlarged pictures showing local free surfaces and smallest dynamic contact angles

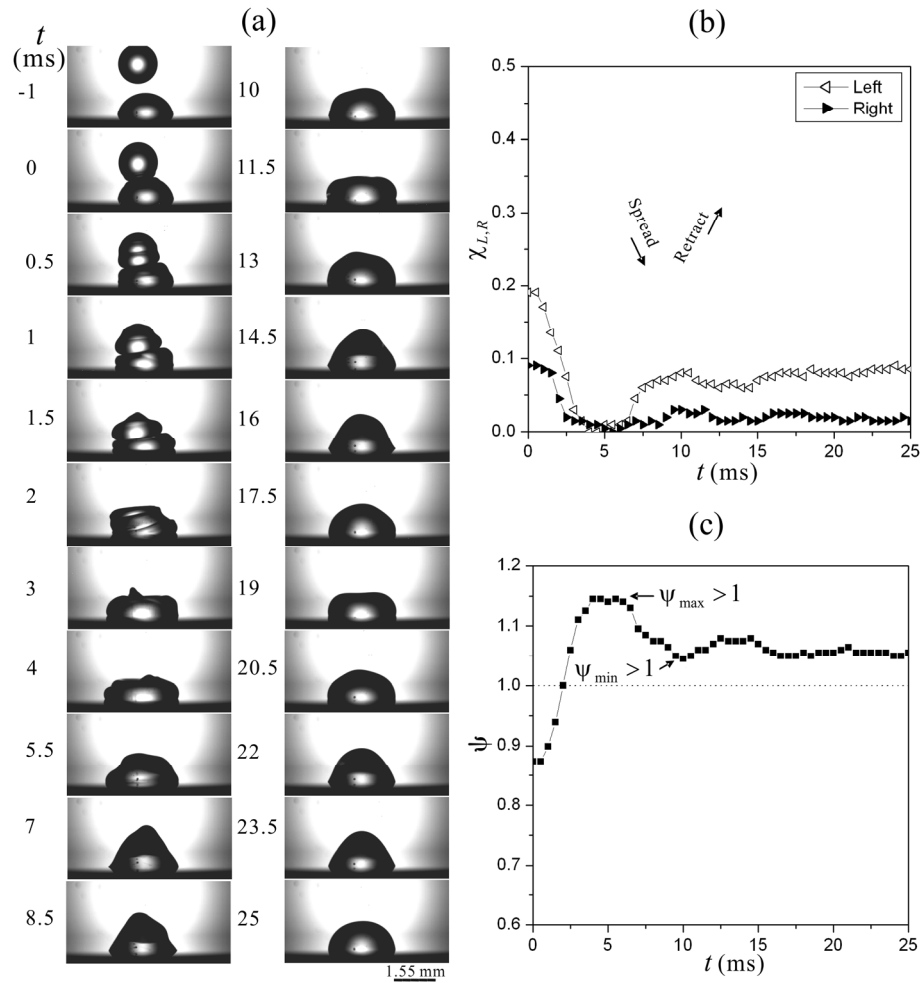


Figure 4: Coalescence of two water droplets on a stainless steel surface ($We=8$, $Re=990$, $\lambda=0.86$): (a) shape evolution; (b) edge displacements; (c) spread length evolution.

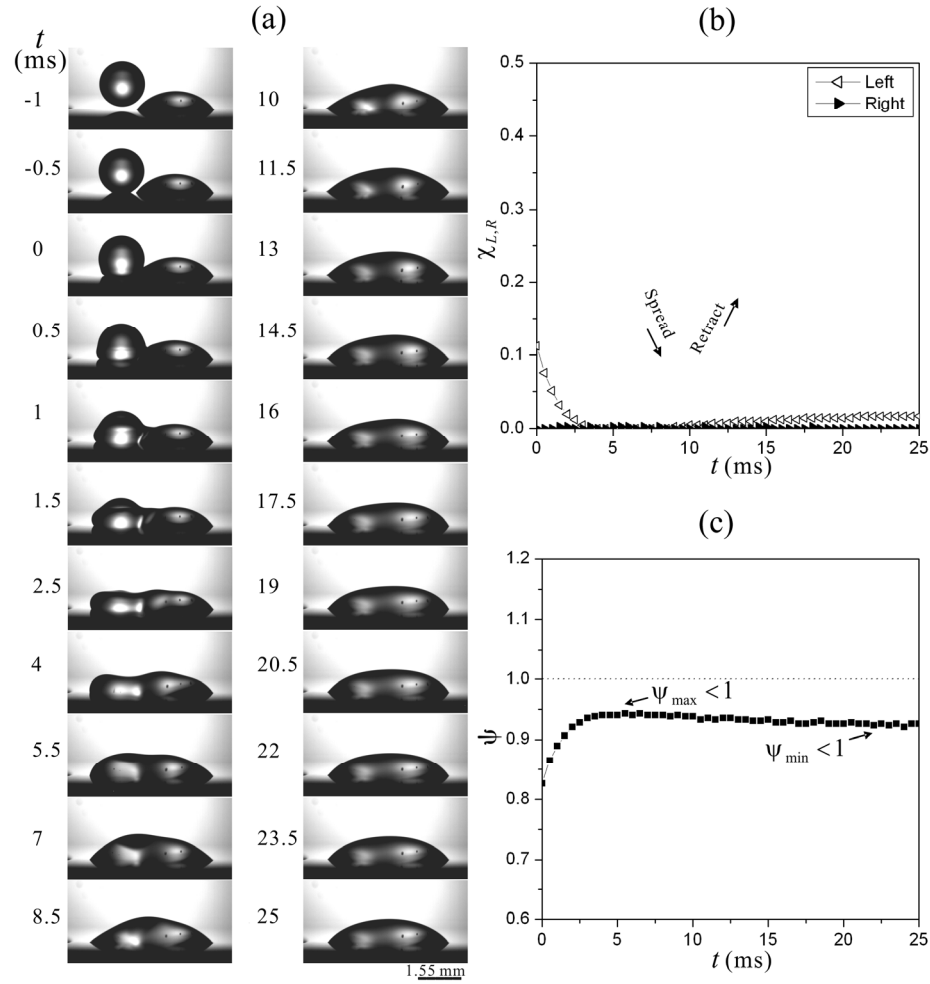


Figure 5: Coalescence of two ethylene glycol droplets on a stainless steel surface ($We=2.4$, $Re=30$, $\lambda=0.31$): (a) shape evolution; (b) edge displacements; (c) spread length evolution.

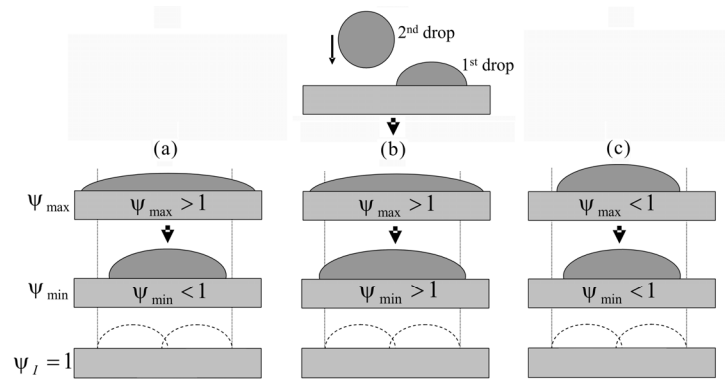


Figure 6: Schematic representation of coalescence mechanisms: (a) drawback due to retraction; (b) additional spread; (c) drawback not due to retraction.